Diphenylamino End-Capped Oligofluorenes with Enhanced Functional Properties for Blue Light Emission: Synthesis and Structure-Property Relationships

ARTICLE *in* CHEMISTRY · MAY 2005

Impact Factor: 5.73 · DOI: 10.1002/chem.200401152 · Source: PubMed

4 AUTHORS, INCLUDING:

Zhong Hui Li,
Chengdu Normal University
36 PUBLICATIONS **863** CITATIONS

SEE PROFILE

Jianping Lu
National Research Council Canada
73 PUBLICATIONS **3,110** CITATIONS

SEE PROFILE

Diphenylamino End-Capped Oligofluorenes with Enhanced Functional Properties for Blue Light Emission: Synthesis and Structure–Property Relationships

Zhong Hui Li,[a] Man Shing Wong,*[a] Ye Tao,*[b] and Jianping Lu[b]

Abstract: A novel series of monodisperse asymmetrically and symmetrically substituted diphenylamino end-capped oligofluorenes, **OF(2)-NPhR**, **R** = **H** or **An** (**An** = 9-anthryl) and **OF(*n*)-NPh**, n = 2–4, has been synthesized by a convergent approach using palladium-catalyzed Suzuki cross-coupling. End-capping of oligofluorenes with diphenylamino group(s) has been shown to offer advantages in terms of lowering their first ionization potentials, enhancing thermal stability, and inducing good amorphous morphological stability. By tuning the number of diphenylamino end-caps and the chain length, the optimal conjugated length for optical and luminescence properties has been determined. Of all the hitherto reported oligofluorenes capable of serving as non-doped blue emitters, **OF(3)-NPh**, with an optimal conjugated length, exhibits some of the best hole-transport and blue-emitting properties. A maximum luminance of 7500 cd m^{-2} and a luminance efficiency up to 1.8 cd A^{-1} have been achieved.

Keywords: cyclic voltammetry · enhanced hole-injection/transport properties · fluorescence · light-emitting materials · oligofluorenes

Introduction

With the advent of first-generation full-color organic light-emitting diode (OLED) displays in consumer electronics, for example in digital cameras and mobile phones, interest in developing highly stable and efficient blue-emissive materials has intensified, as at present these do not match the far superior stabilities and device performances of green-emissive materials.[1,2] Furthermore, good wide-energy-gap emissive materials can be used as host matrices to generate a complete set of primary colors by means of energy transfer to luminescent dopants or by using color filters.[3,4] Fluorene-based molecules[5–7] and polymers,[8–11] which show great promise as highly stable and efficient blue-emissive materials, have been extensively investigated recently. Nevertheless, OLED performance is significantly affected by the charge balance of the injected holes and electrons, as well as by the confinement of carriers and excitons in a device. In addition, a large hole-injection barrier for fluorene-based materials often limits their device efficiency. To improve the hole-injection and transport properties, triarylamines or their moieties have been blended with[12] or incorporated into[13,14] fluorene-based polymers, resulting in greatly enhanced stability and efficiency of blue-emitting OLEDs made with these materials. However, this knowledge does not provide any guidelines for further optimization of fluorene-based materials. Interestingly, there have not been any reports exploring blue-emissive diarylamine- or triarylamine-substituted fluorene-based molecules/oligomers, even though morphologically stable triarylamine derivatives have been widely used as hole-transporting materials.[15,16] Investigations of structure–property relationships in such oligomers can be expected to provide insight into the functional properties of the related polymers as well as useful knowledge for the rational design and optimization of fluorene-based materials. Furthermore, monodisperse functional π-conjugated oligofluorenes with well-defined structure, which can be easily characterized and obtained in high purity, can be utilized as active materials in various optoelectronic applications.

[a] Z. H. Li, Dr. M. S. Wong
Department of Chemistry and Centre for Advanced Luminescence Materials
Hong Kong Baptist University
Kowloon Tong, Hong Kong SAR (China)
Fax: (+852) 3411-7348
E-mail: mswong@hkbu.edu.hk

[b] Dr. Y. Tao, Dr. J. Lu
Institute for Microstructural Sciences
National Research Council of Canada
M-50 Montreal Road, Ottawa, ON, K1A 0R6 (Canada)
Fax: (+1) 613-990-0202
E-mail: ye.tao@nrc.ca

 DOI: 10.1002/chem.200401152

As part of our efforts to investigate the structural factors of functional materials[17–20] that can enhance OLED performance and stability, we report herein the first synthesis of monodisperse diphenylamino end-capped oligofluorenes, **OF(2)-NPhR**, **R** = **H** and **An** and **OF(*n*)-NPh**, n = 2–4,

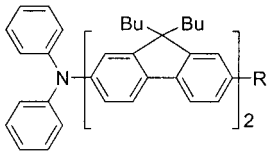

OF(2)-NPhR, R = H or An

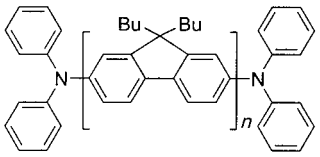

OF(*n*)-NPh, n = 2–4

and an investigation of the influence of diphenylamino end-caps and chain length on various physical and functional properties of oligofluorenes, particularly blue-light-emitting properties. We have unambiguously shown that diphenylamino moieties end-capped onto highly luminescent oligofluorene backbones improve hole-injection/transport properties, induce morphologically stable amorphous thin-film formation, and increase the thermal stability of the oligomers, which makes them superior as difunctional blue-emissive materials. In addition, this systematic investigation has led to the development of an oligofluorene possessing the optimal conjugated length for highly efficient and stable blue emission. Importantly, undoped **OF(3)-NPh**-based multilayer OLEDs exhibit excellent device performance and color chromaticity for practical applications.

Results and Discussion

The syntheses of the monodisperse asymmetrically and symmetrically substituted diphenylamino end-capped oligofluorenes, **OF(2)-NPhR**, **R** = **H** or **An** and **OF(*n*)-NPh**, n = 2–4, are outlined in Scheme 1. Palladium-catalyzed Suzuki cross-coupling was employed to construct the oligofluorene cores, with 9,9-dibutyl-7-(diphenylamino)-2-fluorenylboronic acid (**5**) as a key intermediate in these coupling reactions. Alkylation of fluorene with *n*BuI in the presence of NaOH in DMSO afforded 9,9-dibutylfluorene (**1**) in 82% yield. Monobromination of **1** with *N*-bromosuccinimide (NBS) followed by electrophilic iodination with periodic acid/I_2 afforded 2-bromo-7-iodo-9,9-dibutylfluorene (**3**) in excellent yield (92%). Chemoselective Ullmann coupling of **3** with diphenylamine using Cu/K_2CO_3 in triglyme afforded 2-bromo-7-(diphenylamino)-9,9-dibutylfluorene (**4**), which was subsequently converted to the corresponding boronic acid (**5**) by lithium–bromide exchange with *n*BuLi followed by reaction with trimethyl borate and then acid hydrolysis. Suzuki cross-coupling of boronic acid **5** and bromofluorene **2** using Pd(OAc)$_2$/2P(*o*-tol)$_3$ as catalyst afforded the asymmetrically substituted bifluorene, **OF(2)-NPhH**, in 76% yield. Similarly, cross-coupling of boronic acid **5** and bromide **4** afforded the desired symmetrically substituted bifluorene, **OF(2)-NPh**, in excellent yield (93%) under the same conditions. It is important to note that use of the classical catalyst Pd(PPh$_3$)$_4$ often resulted in a poor yield. Cross-coupling of boronic acid **5** and 7-(9′-anthryl)-2-bromofluorene **7**, which was prepared by selective cross-coupling of 9-anthrylboronic acid (**6**) with 2-bromo-7-iodofluorene (**3**), afforded **OF(2)-NPhAn** in moderate yield (56%). Double palladium-catalyzed cross-coupling of **3** with boronic acid **5** yielded the terfluorene **OF(3)-NPh** in 81% yield. Using the same convergent approach, double palladium-catalyzed cross-coupling of boronic acid **5** and 7,7′-diiodobifluorene **10**, which was synthesized by cross-coupling of **2** and the corresponding fluorenylboronic acid **8** followed by electrophilic iodination, yielded **OF(4)-NPh** in 64% yield. All the newly synthesized oligomers were fully characterized by ^{1}H NMR, ^{13}C NMR, MS, and elemental analysis, and the data were found to be in good agreement with the proposed structures. It is worth mentioning that the protons of the methyl and third methylene groups of the butyl chains attached at the C9 position of fluorene and its derivatives resonate at unexpectedly low frequencies in the ^{1}H NMR spectra. This unusual shift suggests that the methyl and methylene groups fall within the shielding region of the aromatic rings of the fluorene.

To probe the end-capping effect, the corresponding unsubstituted **OF(*n*)** series was also prepared using the same convergent synthetic strategy for comparison. End-capping of one or more diphenylamino functionalities onto oligofluorene cores has pronounced effects on various molecular/functional properties of the oligomers and OLED device performance. In the electronic absorption spectra, a substantial red-shift of the absorption maxima (λ_{max}^{abs}) of oligofluorenes ($\Delta\lambda$ = 25–54 nm) is seen upon incorporation of strongly electron-donating diphenylamino group(s), which is attributed to an asymmetric destabilization of the HOMO and LUMO levels, leading to a decrease in the energy gap.[21] The λ_{max}^{abs} and molar absorptivities (ε_{max}) of both the **OF(*n*)** and **OF(*n*)-NPh** series increase sequentially with increasing chain length; however, λ_{max}^{abs} values of diphenylamino end-capped oligofluorenes show evidence of saturation at 386 nm, even though ε_{max} increases (Figure 1). This implies that an effective conjugated length for the energy gap is reached when n = 3 in the **OF(*n*)-NPh** series. The emission maxima (λ_{max}^{em}) of oligofluorenes consistently shift to longer wavelengths ($\Delta\lambda$ = 22–44 nm) with the incorporation of diphenylamino end-cap(s). Upon excitation at either 310 nm, corresponding to the $n\rightarrow\pi^*$ transition of the triarylamine moiety, or at 386 nm (λ_{max}), corresponding to the $\pi\rightarrow\pi^*$ transition of the oligofluorene core, the emission spectra obtained are identical, suggesting that energy or excitons can be efficiently transfered from the triarylamine moiety to the emissive fluorene core. Consistent with the absorption behavior, the λ_{max}^{em} values of the **OF(*n*)-NPh** series also show a tendency for convergence at 432 nm when n = 3, further supporting the existence of an effective conjugated length for the energy gap (Figure 1).

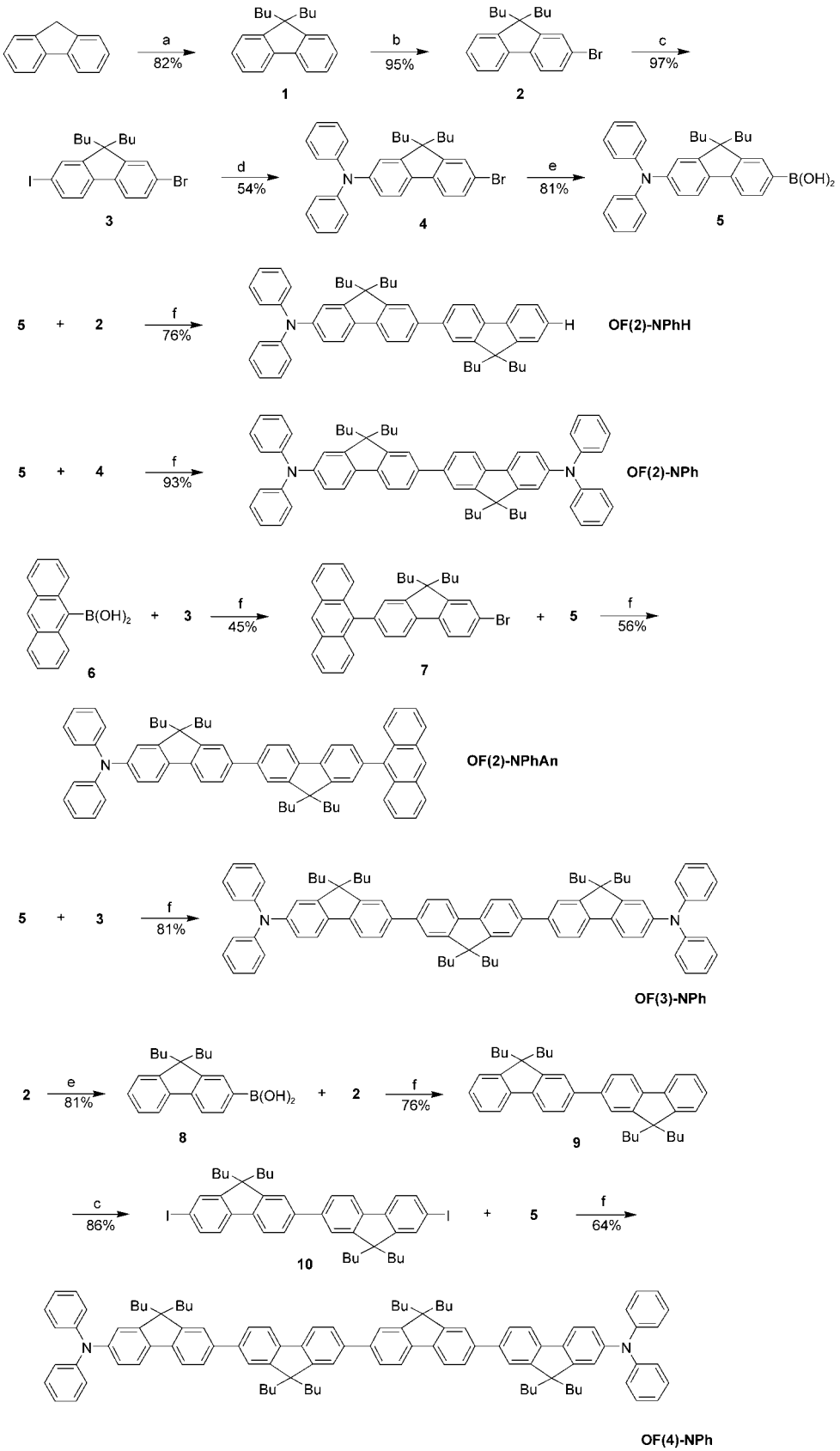

Scheme 1. Synthesis of diphenylamino end-capped oligofluorenes, **OF(2)-NPhR**, **R** = **H** or **An**, and **OF(*n*)-NPh**, n = 2–4. Reagents and conditions: a) *n*BuI, NaOH, DMSO, 90 °C; b) NBS, acetone, 60 °C; c) I_2, HIO_4, AcOH, H_2SO_4, 80 °C; d) Ph_2NH, Cu, K_2CO_3, triglyme, 180 °C; e) 1. *n*BuLi, THF, −78 °C, 2. $B(OCH_3)_3$, 3. H^+; f) $Pd(OAc)_2$/2 P(*o*-tol)$_3$, K_2CO_3, CH_3OH, 75 °C.

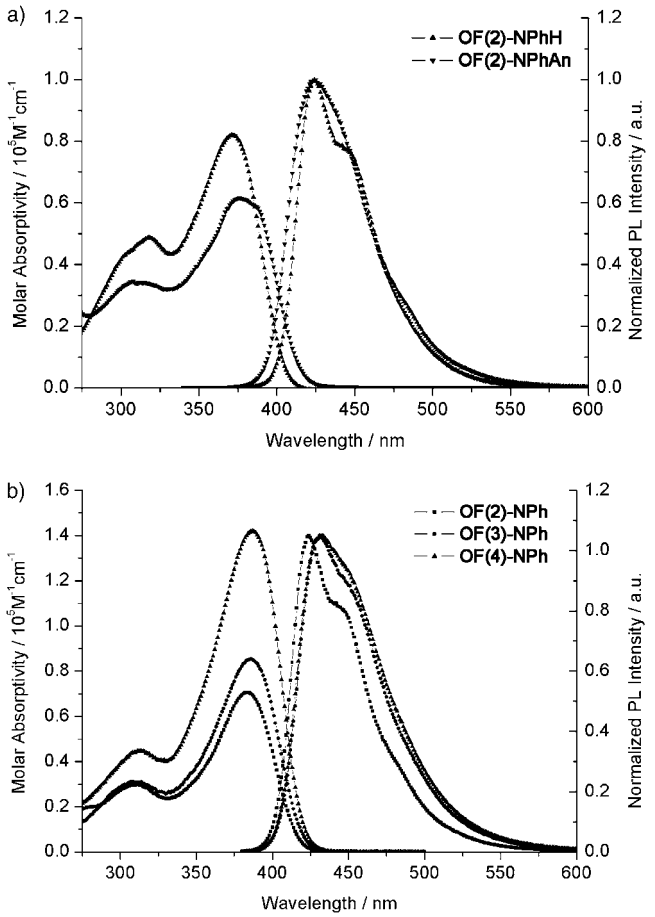

Figure 1. Absorption and fluorescence spectra of the a) **OF(2)-NPhR** and b) **OF(*n*)-NPh** series measured in chloroform.

Importantly, end-capping of one or more diphenylamino functionalities onto the oligofluorene skeleton does not perturb the planarity or alter the highly fluorescent nature of the oligofluorene core (Table 1). The fluorescence quantum yields measured in chloroform using 9,10-diphenylanthracene as a standard increase with increasing chain length and become saturated on reaching the terfluorene ($\Phi_{FL} = 93\%$) in the **OF(*n*)-NPh** series. The fluorescence lifetimes of all the diphenylamino end-capped oligofluorenes are in the nanosecond range, suggesting that the emission originates from a transition between the singlet excited state and the ground state.

To prevent aggregation/excimer formation and to induce an amorphous state for fluorene-based molecular materials, a widely adopted approach is to introduce either a spiro-linkage[22–24] or bulky substituent(s) or dendron(s)[25,26] at the C9-position of the fluorene core. It is important to note that compounds of the **OF(*n*)** series bearing short butyl substituents exhibit no glass transition temperature (T_g), as determined by differential scanning calorimetry (DSC); instead, melting points of 153, 69, and 109 °C were recorded for **OF(2)**, **OF(3)**, and **OF(4)**, respectively, by DSC. On the other hand, oligofluorenes end-capped with diphenylamino group(s) show distinct T_g values, which increase with increasing size of the fluorenyl unit (Table 1). These results suggest that the incorporation of diphenylamino moieties at the ends of oligofluorenes may also be used as a tool to induce morphologically stable amorphous thin-film formation. Furthermore, all of the **OF(2)-NPhR**s and **OF(*n*)-NPh**s show improved thermal stabilities, with decomposition temperatures, T_{dec}, in the range 405–464 °C.

To examine the electrochemical properties of the oligomers, cyclic voltammetry experiments were carried out in a three-electrode cell set-up with 0.1 M Bu_4NPF_4 in CH_2Cl_2 as the supporting electrolyte. The results are tabulated in Table 1. In contrast to the **OF(*n*)** series and triaryldiamines, the asymmetrically substituted bifluorenes, **OF(2)-NPhR**s, exhibit two reversible one-electron anodic redox couples, which correspond to the sequential removal of electrons from the arylamino group and bifluorene core to form radical cations and dications, respectively (Figure 2). One the other hand, the symmetrically disubstituted oligofluorenes, **OF(*n*)-NPh**s, exhibit a reversible two-electron anodic redox couple, corresponding to two arylamine oxidations, as well as a (ir)reversible one-electron anodic redox couple and an additional reversible one-electron redox couple for **OF(4)-**

Table 1. A summary of the various physical measurements on the **OF(2)-NPhR**, **OF(*n*)-NPh**, and **OF(*n*)** series.

	λ_{max}^{abs} [a] [nm] ($\varepsilon_{max}/10^4$ [M^{-1}cm^{-1}])	λ_{max}^{em} [a,b] [nm]	Φ_{FL} [a]	τ [a,e] [ns]	$E_{1/2}$ [f] [V]	HOMO [g] [eV]	T_g [h] [°C]	T_{dec} [i] [°C]
OF(2)-NPhH	372 (4.38)	423	0.50[c]	1.06	0.35, 0.89	5.15	60	406
OF(2)-NPhAn	377 (5.88)	427	0.73[c]	1.48	0.35, 0.78	5.15	93	446
OF(2)-NPh	384 (7.06)	425	0.67[c]	4.56	0.36, 1.06	5.16	91	452
OF(3)-NPh	386 (8.53)	432	0.93[c]	1.23	0.35, 0.87	5.15	99	461
OF(4)-NPh	386 (14.2)	432	0.94[c]	0.92	0.34, 0.79, 0.94	5.14	117	464
OF(2)	330 (4.30)	363, 381	0.71[d]	0.95	0.91, 1.19	5.70	no	369
OF(3)	353 (5.78)	394, 416	0.92[d]	1.04	0.77, 1.01	5.57	no	432
OF(4)	361 (8.23)	410	0.93[d]	0.98	0.73, 0.95	5.53	no	451

[a] Measured in $CHCl_3$. [b] Excited at the absorption maxima. [c] Using 9,10-diphenylanthracene ($\Phi_{360} = 0.9$) as a standard. [d] Using quinine in 1.0 M H_2SO_4 ($\Phi_{313} = 0.48$) as a standard. [e] Using a nitrogen laser as excitation source. [f] $E_{1/2}$ versus Fc^+/Fc estimated by CV using a platinum disc electrode as a working electrode, platinum wire as a counter electrode, and SCE as a reference electrode, connected to the oligomer solution through an agar salt bridge, with ferrocene as an external standard, $E_{1/2}$ (Fc/Fc^+) = 0.45 V versus SCE). [g] Calculated with reference to ferrocene (0.48 eV). [h] Determined by differential scanning calorimetry with a heating rate of 10 °C min^{-1} under N_2. [i] Determined by thermogravimetric analysis with a heating rate of 10 °C min^{-1} under N_2.

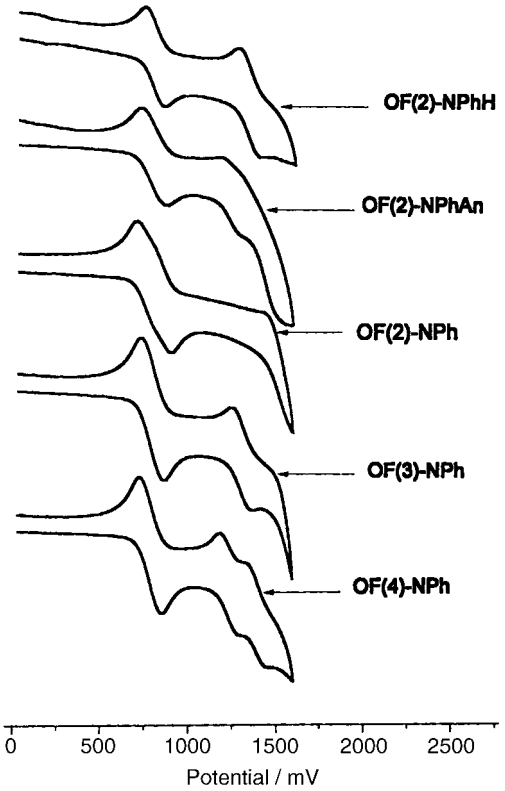

Figure 2. Cyclic voltammograms of the **OF(2)-NPhR** and **OF(*n*)-NPh** series.

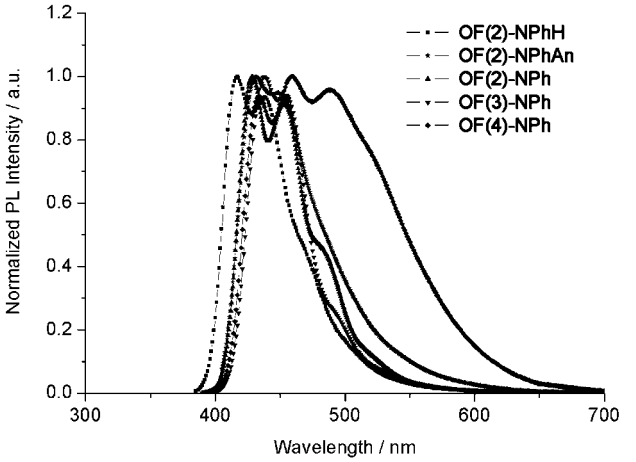

Figure 3. Thin-film photoluminescence spectra of **OF(2)-NPhR**s and **OF(*n*)-NPh**s.

NPh, corresponding to oxidation of the oligofluorene skeleton (Figure 2). The arylamine oxidation potential is essentially unaffected by the number of end-caps and the length of the oligofluorene core; however, the second oxidation proceeds more easily with an increase in conjugated length as the electrochemically formed radical cation is suitably predisposed for efficient delocalization and hence is stabilized. In general, upon the incorporation of diphenylamino end-caps, the HOMO level of oligofluorenes is raised (relative to the vacuum level) to about 5.15 eV, as estimated by electrochemical methods (Table 1). Such a high HOMO level greatly reduces the energy barrier for hole injection from ITO ($\varphi = 5.0$ eV) to the emissive oligofluorenes. As a result, **OF(2)-NPhR**s and **OF(*n*)-NPh**s can also be used as hole-transport/injection materials.

Thin-film photoluminescence (PL) spectra of all of the diphenylamino end-capped oligofluorenes, except **OF(4)-NPh**, show more distinct vibronic structures and slightly red-shifted emission maxima (<6 nm) as compared to the solution PL spectra, indicating the absence of aggregation/excimer formation in the solid state. On the other hand, the significant spectral broadening coupled with a red shift of about 20 nm in the PL spectrum of a vacuum-deposited thin film of **OF(4)-NPh** is indicative of intermolecular interactions between the quaterfluorenyl backbones (Figure 3).

Because of their strong luminescence, low first ionization potentials, high thermal stabilities, and good amorphous morphological stabilities, diphenylamino end-capped oligofluorenes show great potential for use as hole-transport blue-emitters in OLEDs. Multilayer OLEDs with the structure ITO/**OF(2)-NPhR** or **OF(*n*)-NPh** (40 nm)/PBD (40 nm)/LiF (1 nm)/Al (150 nm) were thus fabricated by vacuum deposition and subsequently investigated (PBD = 2-biphenyl-4-yl-5-(4-*tert*-butylphenyl)-1,3,4-oxadiazole). The EL spectra of these devices generally resemble the PL spectra of the thin films, with blue emission maxima at 420–436 nm and a shoulder peak at 456–460 nm (Figure 3, Figure 4a, and Figure 5), with the exception of the EL spectrum of **OF(2)-NPhAn**, which exhibits a tailed emission at long wavelengths. Such a long-wavelength emission may be due to the formation of aggregates, leading to low-energy trapping sites.[27] In addition, these EL spectra proved to be independent of the applied voltage, suggesting that the EL originates purely from the oligomers, without exciplex formation. Importantly, the performance of the device based on the symmetrically disubstituted bifluorene, **OF(2)-NPh**, was found to be superior to those of the devices based on the asymmetrically substituted bifluorenes, **OF(2)-NPhAn** and **OF(2)-NPhH** (Figure 4), even though the systems possess comparable molecular properties, such as hole-injection and transport properties as well as fluorescence quantum yield. As a result, further studies of device performance were concentrated on the **OF(*n*)-NPh** materials.

Over a wide operation range, the emission of **OF(2)-NPh**-based devices was found to have CIE coordinates (x, y = 0.15, 0.09) very close to those of NTSC blue (x, y = 0.14, 0.08). The emission of **OF(3)-NPh**-based devices has CIE coordinates (x, y = 0.16, 0.14), which are also very close to those of NTSC blue.

Despite the fact that the **OF(2)-NPh**-based devices exhibited a turn-on voltage of 4.5 V, a maximum luminance of 1000 cd m^{-2}, and a luminance efficiency up to 1.1 cd A^{-1}, and the **OF(3)-NPh**-based device exhibited a turn-on voltage of 4.5 V, a maximum luminance of 700 cd m^{-2}, and a luminance efficiency up to 2.2 cd A^{-1}, these devices broke down at around 15–16 V (Figure 6). The breakdown of these PBD-

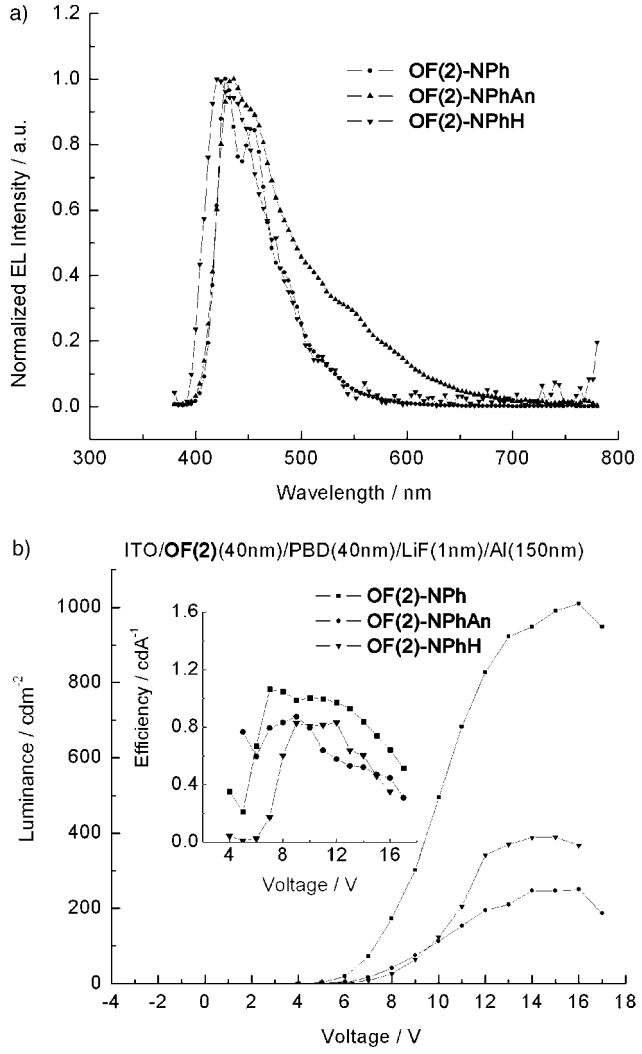

Figure 4. a) EL spectra of **OF(2)-NPhR**- and **OF(2)-NPh**-based devices and b) luminance–voltage plots of **OF(2)-NPhR**- and **OF(2)-NPh**-based devices. The inset shows plots of external efficiency versus voltage.

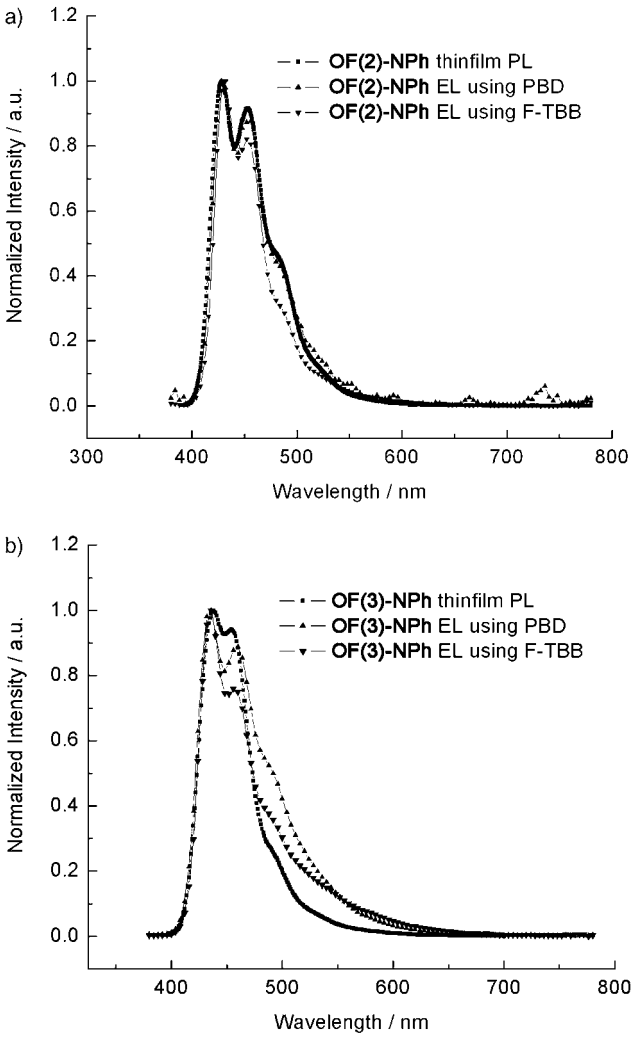

Figure 5. PL spectra of a) **OF(2)-NPh** and b) **OF(3)-NPh**, as well as EL spectra of the corresponding OLEDs.

based devices at high current is most probably due to the poor morphological stability of the PBD film at device operating temperatures. To further enhance the device performance, a hole-blocking amorphous material, 1,3,5-tris(4-fluorobiphenyl-4′-yl)benzene (F-TBB),[28] combined with an Alq_3 film as a hole-blocking/electron-transport layer, was used to replace the PBD layer. The EL spectra of the resulting devices showed no apparent difference from those obtained using the PBD layer (Figure 5). The CIE coordinates of the **OF(2)-NPh**- and **OF(3)-NPh**-based devices using F-TBB as the hole-blocking layer were found to be $x, y =$ 0.16, 0.08, and $x, y =$ 0.17, 0.14, respectively. Remarkably, the **OF(*n*)-NPh**-based devices could be operated at much higher current/voltage with the use of the F-TBB layer, resulting in a much higher maximum luminance than could be achieved with a PBD layer (Figure 6). As a result, the **OF(2)-NPh**-based devices exhibited a maximum luminance of 6000 cd m^{-2} and a luminance efficiency of up to 0.8 cd A^{-1}, whereas the **OF(3)-NPh**-based devices exhibited a maximum luminance of 7500 cd m^{-2} and a luminance efficiency of up to 1.8 cd A^{-1}. Both devices have a turn-on voltage of 7.5 V. The superior device performance of the **OF(3)-NPh**-based OLED is attributed to the significantly higher fluorescence quantum, F_{FL}, of **OF(3)-NPh** (0.93) compared to that of **OF(2)-NPh** (0.67). The HOMO levels of F-TBB (6.3 eV) and PBD (6.2 eV) are very close, but the LUMO level of F-TBB (2.4 eV) is much higher than that of PBD (2.8 eV). Therefore, one trade-off resulting from the use of F-TBB to obtain higher luminance is increased turn-on voltages and slightly decreased device efficiencies.

In summary, a novel series of monodisperse asymmetrically and symmetrically substituted diphenylamino end-capped oligofluorenes, **OF(2)-NPhR**, **R** = **H** or **An** and **OF(*n*)-NPh**, $n =$ 2–4, has been successfully synthesized by a convergent approach using palladium-catalyzed Suzuki cross-coupling. We have shown that terfluorene symmetrically end-capped with diphenylamino groups, **OF(3)-NPh**, possesses the optimal conjugated length for optical and lumi-

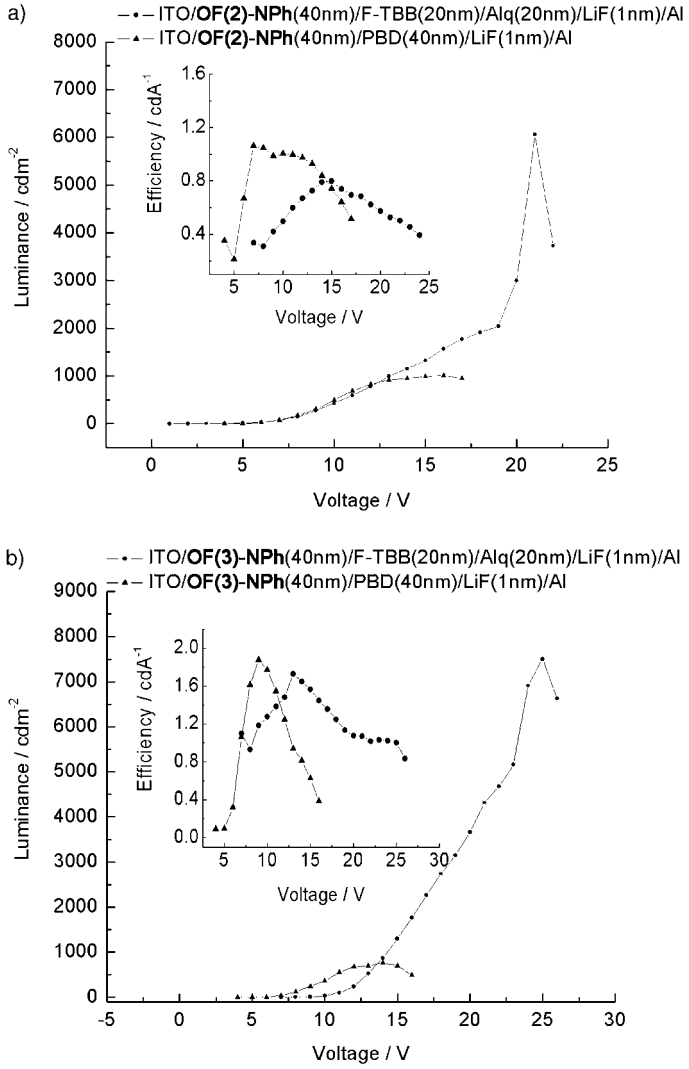

Figure 6. Luminance–voltage plots of a) **OF(2)-NPh**- and b) **OF(3)-NPh**-based devices. The inset shows plots of external efficiency versus voltage.

nescence properties in this series. The diphenylamino end-caps do not perturb the planarity or alter the highly fluorescent nature of the oligofluorene backbone, although the absorption and emission spectra are red-shifted (20–50 nm). Furthermore, the presence of diphenylamino end-caps lowers the first ionization potential (raises the HOMO level of oligofluorenes to ~5.15 eV), as estimated by cyclic voltammetry experiments, which greatly reduces the energy barrier for hole injection from ITO to the emissive oligofluorenes. Diphenylamino end-capped oligofluorenes show enhanced thermal stability and exhibit superior amorphous morphological stability as compared to those of the corresponding unsubstituted counterparts. Remarkably, undoped **OF(*n*)-NPh**-based multilayer OLEDs exhibit excellent device performance and color chromaticity. Depending on the hole-blocking material used (i.e., PBD or 1,3,5-tris(4-fluorobiphenyl-4′-yl)benzene (F-TBB)), the **OF(2)-NPh**-based devices exhibited a maximum luminance of 1000–6000 cd m^{-2} and a luminance efficiency up to 0.8–1.1 cd A^{-1}, whereas the **OF(3)-NPh**-based device exhibited a maximum luminance of 700–7500 cd m^{-2} and a luminance efficiency up to 1.8–2.2 cd A^{-1}. Our findings provide a useful alternative approach to the design of stable and efficient blue-emissive materials.

Experimental Section

EL device fabrication and testing: ITO-glass substrates (15 Ω m^{-2}) were patterned by applying conventional photolithography techniques with an acid mixture of HCl and HNO_3 as the etchant. The active area of each EL device was 1×5 mm^2. All organic layers were thermally deposited in a vacuum chamber at a base pressure of 2×10^{-7} Torr. Typically, a diphenylamino end-capped oligofluorene (**OF(*n*)-NPh**), functioning as a hole-transport emissive layer (40 nm), was first deposited on a patterned ITO substrate. A hole-blocking layer (F-TBB, 20 nm) was then vacuum-deposited on top of the oligofluorene layer, followed by the deposition of an Alq_3 thin film (20 nm). The device fabrication was completed by the evaporation of LiF (1 nm) and the Al cathode (100 nm). A film of PBD (40 nm) was used to replace the F-TBB (20 nm) and Alq_3 (20 nm) in some devices for comparison purposes. The devices were tested in air under ambient conditions with no encapsulation. EL spectra, device luminances, and current–voltage characteristics were recorded using a combination of a Photo Research PR-650 SpectraScan and a Keithley 238 Source meter.

9,9-Bis(*n*-butyl)fluorene (1): A mixture of fluorene (16.6 g, 0.1 mol), *n*-butyl iodide (40 g, 0.22 mol), and sodium hydroxide (12 g, 0.3 mol) in DMSO (120 mL) was stirred overnight at 90 °C under an inert atmosphere. After cooling to room temperature, the solution was poured into cold water and the resulting mixture was extracted with dichloromethane (3×50 mL). The combined organic layers were washed with water, dried over anhydrous sodium sulfate, filtered, and concentrated to dryness. The crude product was then purified by column chromatography on silica gel using petroleum ether as eluent to afford the desired product as a colorless solid (23 g, 82% yield). ^{1}H NMR (400 MHz, $CDCl_3$, 25 °C): δ = 7.70–7.69 (m, 2H; ArH), 7.28–7.33 (m, 6H; ArH), 1.94–1.98 (m, 4H; CH_2), 1.03–1.09 (m, 4H; CH_2), 0.66 (t, J (H,H) = 7.4 Hz, 6H; CH_3), 0.54–0.62 ppm (m, 4H; CH_2); ^{13}C NMR (100 MHz, $CDCl_3$, 25 °C): δ = 150.6, 141.1, 127.0, 126.7, 122.8, 119.6, 54.9, 40.2, 25.9, 23.0, 13.8 ppm; MS (FAB): m/z: 280.2 [M^+].

9,9-Bis(*n*-butyl)-2-bromofluorene (2): A mixture of 9,9-bis(*n*-butyl)fluorene (13 g, 46 mmol) and NBS (8.25 g, 46 mmol) in acetone (50 mL) was stirred under nitrogen at 80 °C for 3 h. After cooling to room temperature, the solution was poured into cold water and the resulting mixture was extracted with dichloromethane (3×50 mL). The combined organic layers were washed with water, dried over anhydrous sodium sulfate, filtered, and concentrated to dryness. The crude product was purified by short-column chromatography on silica gel using petroleum ether as eluent to afford the desired product as a colorless solid (15.78 g, 96% yield). ^{1}H NMR (400 MHz, $CDCl_3$, 25 °C): δ = 7.64–7.66 (m, 1H; ArH), 7.50–7.55 (m, 1H; ArH), 7.42–7.45 (m, 2H; ArH), 7.31–7.33 (m, 3H; ArH), 1.89–1.98 (m, 4H; CH_2), 1.02–1.10 (m, 4H; CH_2), 0.67 (t, J(H,H) = 7.4 Hz, 6H; CH_3), 0.51–0.62 ppm (m, 4H; CH_2); ^{13}C NMR (100 MHz, $CDCl_3$, 25 °C): δ = 152.9, 150.3, 140.1, 140.0, 129.9, 127.4, 126.9, 126.7, 126.1, 122.9, 121.0, 119.7, 55.3, 40.1, 25.8, 23.0, 13.8 ppm; MS (FAB): m/z: 359.5 [M^+].

9,9-Bis(*n*-butyl)-2-bromo-7-iodofluorene (3): A mixture of 9,9-bis(*n*-butyl)-2-bromofluorene (15.4 g, 43 mmol), iodine (6.5 g, 25.8 mmol), concentrated sulfuric acid (2.3 mL), periodic acid (1.7 g, 25.8 mmol), and water (7.7 mL) in glacial acetic acid (74 mL) was stirred at 50 °C for 4 h. After cooling to room temperature, the solution was poured into ice-cooled water containing a large amount of sodium sulfite and the resulting mixture was extracted with dichloromethane (3×50 mL). The combined organic phases were washed twice with water, dried over anhydrous sodium sulfate, and concentrated to dryness. The crude product

was purified by short-column chromatography on silica gel using petroleum ether as eluent to yield the desired product as a light-yellow solid (20.3 g, 97% yield). ^{1}H NMR (400 MHz, $CDCl_3$, 25°C): δ = 7.62–7.65 (m, 2H; ArH), 7.49–7.51 (m, 1H; ArH), 7.38–7.44 (m, 3H; ArH), 1.86–1.91(m, 4H; CH_2), 1.02–1.11 (m, 4H; CH_2), 0.67 (t, J(H,H) = 7.2 Hz, 6H; CH_3), 0.50–0.58 ppm (m, 4H; CH_2); ^{13}C NMR (100 MHz, $CDCl_3$, 25°C): δ = 152.7, 152.5, 152.3, 139.7, 139.1, 136.0, 132.1, 132.1, 132.0, 130.1, 130.1, 126.1, 121.5, 121.2, 93.0, 55.5, 40.0, 25.8, 22.9, 13.8 ppm; MS (FAB): m/z: 485.5 [M^+].

9,9-Bis(*n*-butyl)-7-bromo-2-diphenylaminofluorene (4): A mixture of 9,9-bis(*n*-butyl)-2-bromo-7-iodofluorene (10.0 g, 20.6 mmol), diphenylamine (4.2 g, 24.7 mmol), copper bronze (0.7 g, 11 mmol), and potassium carbonate (11 g, 82.4 mmol) in triglyme (50 mL) was stirred under an inert atmosphere at 190–200°C for 24 h. After cooling to room temperature, the solution was poured into cold water and the resulting mixture was extracted with dichloromethane (3×50 mL). The combined organic phases were washed with water, dried over anhydrous sodium sulfate, and concentrated to dryness. The crude product was purified by short-column chromatography on silica gel using petroleum ether as eluent to afford the desired product as a white solid (5.8 g, 54% yield), along with 2,7-bis(diphenylamino)-9,9-di(*n*-butyl)fluorene as a white solid (2.0 g, 26%). ^{1}H NMR (400 MHz, $CDCl_3$, 25°C): δ = 7.38–7.51 (m, 4H; ArH), 7.21–7.25 (m, 4H; ArH), 7.06–7.11 (m, 5H; ArH), 6.98–7.01 (m, 3H; ArH), 1.79–1.83 (m, 4H; CH_2), 1.02–1.09 (m, 4H; CH_2), 0.69 (t, J(H,H) = 7.4 Hz, 6H; CH_3), 0.58–0.64 ppm (m, 4H; CH_2); ^{13}C NMR (100 MHz, $CDCl_3$, 25°C): δ = 152.8, 151.7, 147.9, 147.5, 140.0, 135.0, 129.9, 129.2, 126.0, 123.9, 123.3, 122.6, 120.4, 120.1, 119.0, 55.2, 39.9, 25.9, 22.9, 13.8 ppm; MS (FAB): m/z: 525.4 [M^++H].

9,9-Bis(*n*-butyl)-2-diphenylamino-7-fluorenylboronic acid (5): A 100-mL two-necked flask was charged with a solution of 9,9-bis(*n*-butyl)-7-bromo-2-diphenylaminofluorene (1.3 g, 2.47 mmol) in dry THF (20 mL) and a magnetic stirrer bar. The solution was cooled to −78°C by immersing the flask in an acetone/dry ice bath, whereupon *n*BuLi (1.5 M, 2.3 mL, 3.71 mmol) was added under nitrogen atmosphere while maintaining good stirring. After stirring for 1 h, trimethyl borate (0.4 mL, 3.71 mmol) was added. After stirring for a further 2 h, the reaction mixture was first quenched with water and then 6 M HCl was added in a dropwise fashion until an acidic solution was obtained. The resulting mixture was poured into water and extracted with dichloromethane (3×50 mL). The combined organic layers were dried over anhydrous Na_2SO_4 and concentrated to dryness. The crude product was then purified by column chromatography on silica gel using CH_2Cl_2/EtOAc as eluent to afford the desired boronic acid as a light-yellow solid (976 mg, 81% yield). ^{1}H NMR (400 MHz, [D_6]DMSO, 25°C): δ = 8.02 (s, 2H; OH), 7.79 (s, 1H; ArH), 7.75 (d, J(H,H) = 7.6 Hz, 1H; ArH), 7.70 (d, J(H,H) = 8.0 Hz, 1H, ArH), 7.65 (d, J(H,H) = 8.4 Hz, 1H), 7.26 (t, J(H,H) = 7.4 Hz, 4H; ArH), 7.08 (s, 1H; ArH), 7.00 (d, J(H,H) = 8.0 Hz, 6H; ArH), 6.92 (d, J(H,H) = 8.0 Hz, 1H; ArH), 1.83–1.85 (m, 4H; CH_2), 0.99–1.03 (m, 4H; CH_2), 0.63 (t, J(H,H) = 7.4 Hz, 6H; CH_3), 0.49–0.55 ppm (m, 4H; CH_2); ^{13}C NMR (100 MHz, $CDCl_3$, 25°C): δ = 153.1, 150.0, 147.9, 145.3, 135.6, 134.7, 129.4, 129.2, 124.0, 123.9, 123.2, 122.7, 121.1, 119.0, 118.6, 54.9, 39.9, 26.0, 23.0, 13.8 ppm; MS (FAB): m/z: 489.7 [M^+].

2,2′-Bis(diphenylamino)bis[9,9-bis(*n*-butyl)fluorene], OF(2)-NPh: A 100-mL round-bottomed flask was charged with a mixture of 9,9-bis(*n*-butyl)-7-bromo-2-diphenylaminofluorene (262 mg, 0.50 mmol), 9,9-bis(*n*-butyl)-2-diphenylamino-7-fluorenylboronic acid (347 mg, 0.70 mmol), $Pd(OAc)_2$ (11 mg, 5 mol%), and tri(*o*-tolyl)phosphine (30 mg, 10 mol%), which was taken up in toluene (20 mL), methanol (10 mL), and 2 M aqueous K_2CO_3 solution (2 mL). The reaction mixture was stirred overnight at 75°C under a nitrogen atmosphere. After cooling to room temperature, it was poured into cold water and the resulting mixture was extracted with dichloromethane (3×50 mL). The combined organic layers were dried over anhydrous Na_2SO_4 and concentrated to dryness. The crude product was purified by column chromatography on silica gel using petroleum ether/dichloromethane (6:1, *v*/*v*) as eluent to afford the desired product as a yellow solid (414 mg, 93% yield). ^{1}H NMR (400 MHz, $CDCl_3$, 25°C): δ = 7.69 (d, J(H,H) = 7.6 Hz, 2H; ArH), 7.63 (d, J(H,H) = 8.0 Hz, 2H; ArH), 7.59–7.61 (m, 4H; ArH), 7.27 (d, J(H,H) = 8.0 Hz, 8H; ArH), 7.15 (d, J(H,H) = 7.6 Hz, 10H; ArH), 7.00–7.06 (m, 6H; ArH), 1.88–1.99 (m, 8H; CH_2), 1.07–1.15 (m, 8H; CH_2), 0.73 ppm (t, J(H,H) = 7.4 Hz, 20H; CH_2CH_3); ^{13}C NMR (100 MHz, $CDCl_3$, 25°C): δ = 119.3, 152.4, 151.4, 148.0, 147.1, 140.0, 139.6, 136.0, 129.1, 125.9, 123.8, 123.5, 122.5, 121.0, 120.3, 119.4, 55.1, 40.0, 26.1, 23.0, 13.9 ppm; MS (FAB): m/z: 889.0 [M^+]; elemental analysis calcd (%) for $C_{66}H_{68}N_2$ (888.5382): C 89.14, H 7.71, N 3.15; found: C 88.82, H 7.72, N 3.29.

2-(Diphenylamino)bis[9,9-bis(*n*-butyl)fluorene], OF(2)-NPhH: The Suzuki coupling procedure described above was followed using 9,9-bis(*n*-butyl)-2-bromofluorene (359 mg, 1 mmol) and 9,9-bis(*n*-butyl)-2-diphenylamino-7-fluorenylboronic acid (489 mg, 1 mmol). The crude product was purified by column chromatography on silica gel using petroleum ether/dichloromethane (6:1, v/v) as eluent to afford a light-yellow solid (549 mg, 76% yield). ^{1}H NMR (400 MHz, $CDCl_3$, 25°C): δ = 7.80 (d, J(H,H) = 7.60 Hz, 1H; ArH), 7.76 (d, J(H,H) = 7.20 Hz, 1H; ArH), 7.72 (d, J(H,H) = 8.40 Hz, 1H; ArH), 7.69–7.61 (m, 5H; ArH), 7.40–7.33 (m, 3H; ArH), 7.28 (t, J(H,H) = 7.20 Hz, 4H; ArH), 7.17 (d, J(H,H) = 7.60 Hz, 5H; ArH), 7.09–7.02 (m, 3H; ArH), 2.08–1.92 (m, 8H; CH_2), 1.16–1.09 (m, 8H; CH_2), 0.77–0.70 ppm (m, 20H; CH_2CH_3); ^{13}C NMR (100 MHz, $CDCl_3$, 25°C): δ = 152.4, 151.4, 151.3, 150.9, 148.0, 147.1, 140.8, 140.4, 140.2, 140.1, 139.6, 135.9, 129.1, 126.9, 126.8, 126.0, 125.9, 123.8, 123.5, 122.9, 122.5, 121.2, 121.1, 120.4, 119.9, 119.7, 119.4, 119.3, 55.1, 40.2, 40.0, 26.1, 26.0, 23.1, 23.0, 13.9, 13.8 ppm; MS (FAB): m/z = 722.0 [M^+]; elemental analysis calcd (%) for $C_{54}H_{59}N$ (721.4647): C 89.82, H 8.24, N 1.94; found: C 89.98, H 8.30, N 1.89.

9,9-Bis(*n*-butyl)-7-(9′-anthryl)-2-bromofluorene (7): The Suzuki coupling procedure described above was followed using 9,9-bis(*n*-butyl)-2-bromo-7-iodofluorene (971 mg, 2 mmol) and 9-anthrylboronic acid (444 mg, 2 mmol). The crude product was purified by column chromatography on silica gel using petroleum ether as eluent to afford a light-yellow solid (480 mg, 45% yield) and the di-coupling product in 35% yield. ^{1}H NMR (400 MHz, $CDCl_3$, 25°C): δ = 8.51 (s, 1H; ArH), 8.06 (d, J(H,H) = 8.40 Hz, 2H; ArH), 7.87 (d, J(H,H) = 8.40 Hz, 1H; ArH), 7.72 (t, J(H,H) = 4.40 Hz, 2H; ArH), 7.66 (d, J(H,H) = 8.80 Hz, 1H; ArH), 7.52–7.32 (m, 8H; ArH), 1.99–1.95 (m, 4H; CH_2), 1.15–1.06 (m, 4H; CH_2), 0.78–0.67 ppm (m, 10H; CH_2CH_3); ^{13}C NMR (100 MHz, $CDCl_3$; 25°C): δ = 152.9, 150.3, 140.1, 140.0, 138.3, 138.0, 136.4, 131.8, 131.3, 130.1, 129.8, 127.4, 126.9, 126.1, 126.0, 122.8, 121.1, 121.0, 120.9, 119.7, 55.2, 40.1, 25.8, 22.9, 13.8 ppm; MS (FAB): m/z: 534.5 [M^++H].

9-[7-(2′-Diphenylamino-bi(9,9-bis(*n*-butyl)fluorene))-yl]anthracene, OF(2)-NPhAn: The Suzuki coupling procedure described above was followed using 9,9-bis(*n*-butyl)-7-(9′-anthryl)-2-bromofluorene (267 mg, 0.5 mmol) and 9,9-bis(*n*-butyl)-2-diphenylamino-7-fluorenylboronic acid (367 mg, 0.75 mmol). The crude product was purified by column chromatography on silica gel using petroleum ether/dichloromethane (6:1, v/v) as eluent to afford a yellow solid (251 mg, 56% yield). ^{1}H NMR (400 MHz, $CDCl_3$, 25°C): δ = 8.52 (s, 1H; ArH), 8.07 (d, J(H,H) = 8.0 Hz, 2H; ArH), 7.94 (d, J(H,H) = 7.60 Hz, 1H; ArH), 7.88 (d, J(H,H) = 7.60 Hz, 1H; ArH), 7.79 (d, J(H,H) = 9.20 Hz, 2H; ArH), 7.73–7.67 (m, 3H; ArH), 7.63 (s, 1H; ArH), 7.60 (d, J(H,H) = 8.40 Hz, 2H; ArH), 7.49–7.42 (m, 4H; ArH), 7.36 (dd, J(H,H) = 7.60 Hz, 2H; ArH), 7.26 (d, J(H,H) = 7.60 Hz, 4H; ArH), 7.16 (s, 5H; ArH), 7.06–7.01 (m, 3H; ArH), 2.08–1.91 (m, 8H; CH_2), 1.16–1.09 (m, 8H; CH_2), 0.76–0.70 ppm (m, 20H; CH_2CH_3); ^{13}C NMR (100 MHz, $CDCl_3$, 25°C): δ = 152.3, 151.6, 151.3, 151.0, 147.9, 147.1, 140.5, 140.1, 140.0, 137.9, 137.5, 137.2, 136.7, 131.3, 130.2, 129.9, 129.1, 128.3, 126.8, 126.4, 126.1, 126.0, 125.2, 125.0, 123.8, 122.4, 121.2, 120.3, 119.9, 119.5, 119.3, 55.3, 55.2, 40.2, 40.1, 26.3, 26.2, 23.1, 23.0, 14.2, 14.0 ppm; MS (FAB): m/z: 898.0 [M^+]; elemental analysis calcd (%) for $C_{68}H_{67}N$ (897.5273): C 90.92, H 7.52, N 1.56; found: C 91.25, H 7.68, N 1.65.

2,2″-Bis(diphenylamino)tris[9,9-bis(*n*-butyl)fluorene], OF(3)-NPh: The Suzuki coupling procedure described above was followed using 9,9-bis(*n*-butyl)-2-bromo-7-iodofluorene (734 mg, 1.5 mmol) and 9,9-bis(*n*-butyl)-2-diphenylamino-7-fluorenylboronic acid (2.20 g, 4.5 mmol). The crude product was purified by column chromatography on silica gel using petroleum ether/dichloromethane (6:1, v/v) as eluent to afford a light-yellow solid (944 mg, 81% yield). ^{1}H NMR (400 MHz, $CDCl_3$, 25°C): δ = 7.80 (d, J(H,H) = 8.0 Hz, 2H; ArH), 7.63–7.70 (m, 8H; ArH), 7.58–

7.60 (m, 4H; ArH), 7.25 (d, J(H,H) = 8.0 Hz, 8H; ArH), 7.14 (d, J-(H,H) = 7.6 Hz, 10H; ArH), 6.99–7.05 (m, 6H; ArH), 2.09–2.11 (m, 4H; CH_2), 1.90–1.98 (m, 8H; CH_2), 1.10–1.18 (m, 12H; CH_2), 0.71–0.75 ppm (m, 30H; CH_2CH_3); ^{13}C NMR (100 MHz, $CDCl_3$, 25 °C): δ = 152.4, 151.7, 151.4, 148.0, 147.1, 140.4, 140.2, 139.9, 139.6, 135.9, 129.1, 126.0, 123.8, 123.5, 122.5, 121.3, 121.2, 120.4, 119.9, 119.4, 119.3, 55.2, 55.1, 40.2, 40.0, 26.1, 23.1, 23.0, 13.9, 13.8 ppm; MS (FAB): m/z: 1165.4 [M^+]; elemental analysis calcd (%) for $C_{87}H_{92}N_2$ (1164.7260): C 89.64, H 7.95, N 2.41; found: C 89.40, H 8.15, N 2.65.

9,9-Bis(*n*-butyl)-2-fluorenylboronic acid (8): The procedure described for **5** was followed by using 9,9-bis(*n*-butyl)-2-bromofluorene (7.9 g, 22 mmol), *n*BuLi (16.5 mL, 26.4 mmol), and trimethyl borate (3.0 mL, 26.4 mmol), affording a light-yellow solid in an isolated yield of 81%. ^{1}H NMR (400 MHz, [D$_6$]DMSO, 25 °C): δ = 8.05 (s, 2H; OH), 7.83 (s, 1H; ArH), 7.74–7.81 (m, 3H; ArH), 7.42–7.44 (m, 1H; ArH), 7.31–7.33 (m, 2H; ArH), 1.95–1.98 (m, 4H; CH_2), 0.98–1.04 (m, 4H; CH_2), 0.60 (t, J-(H,H) = 7.4 Hz, 6H; CH_3), 0.43–0.48 ppm (m, 4H; CH_2); ^{13}C NMR (100 MHz, [D$_6$]DMSO, 25 °C): δ = 150.6, 148.9, 142.4, 140.5, 133.0, 128.3, 127.5, 126.8, 122.9, 121.1, 118.8, 54.3, 40.1, 25.8, 22.5, 13.8 ppm.

Bis[9,9-bis(*n*-butyl)fluorene] (9): The Suzuki coupling procedure described above was followed using 2-bromo-9,9-bis(*n*-butyl)fluorene (1.0 g, 2.78 mmol), 9,9-bis(*n*-butyl)-2-fluorenylboronic acid (897 mg, 2.78 mmol), $Pd(OAc)_2$ (31 mg, 5 mol%), and tri(*o*-tolyl)phosphine (85 mg, 10 mol%). The crude product was purified by column chromatography on silica gel using petroleum ether as eluent to afford the desired product as a white solid (1.02 g, 76% yield). ^{1}H NMR (400 MHz, $CDCl_3$, 25 °C): δ = 7.71–7.78 (m, 4H; ArH), 7.61–7.65 (m, 4H; ArH), 7.32–7.36 (m, 6H; ArH), 1.99–2.06 (m, 8H; CH_2), 1.06–1.14 (m, 8H; CH_2), 0.64–0.71 ppm (m, 20H; CH_2CH_3); ^{13}C NMR (100 MHz, $CDCl_3$, 25 °C): δ = 151.3, 150.8, 140.6, 140.3, 140.2, 126.9, 126.7, 125.9, 122.8, 121.2, 119.8, 119.6, 55.1, 40.3, 26.1, 23.2, 13.9 ppm; MS (FAB): m/z: 554.6 [M^+]; elemental analysis calcd (%) for $C_{42}H_{50}$ (554.3912): C 90.92, H 9.08; found: C 90.73, H 8.98.

2,2′-Diiodo-bis[9,9-bis(*n*-butyl)fluorene] (10): The iodination procedure described for the preparation of **3** was followed using bis[9,9-bis(*n*-butyl)-2-bromofluorene] (816 mg, 1.47 mmol), iodine (410 mg, 1.62 mmol), concentrated sulfuric acid (2.0 mL), water (2.0 mL), and periodic acid (456 mg, 1.62 mmol). The crude product was purified by column chromatography on silica gel using petroleum ether as eluent to afford the desired product as a white solid (1.01 g, 86% yield). ^{1}H NMR (400 MHz, $CDCl_3$, 25 °C): δ = 7.74 (d, J(H,H) = 8.0 Hz, 2H; ArH), 7.61–7.68 (m, 6H; ArH), 7.57 (s, 2H; ArH), 7.47 (d, J(H,H) = 8.4 Hz, 2H; ArH), 1.92–2.06 (m, 8H; CH_2), 1.06–1.15 (m, 8H; CH_2), 0.61–0.71 ppm (m, 20H; CH_2CH_3); ^{13}C NMR (100 MHz, $CDCl_3$, 25 °C): δ = 153.4, 150.9, 140.8, 140.3, 139.4, 135.9, 132.1, 126.2, 121.5, 121.3, 120.1, 92.5, 55.3, 40.1, 25.9, 23.0, 13.8 ppm; MS (FAB): m/z: 806.5 [M^+].

2,2″-Bis(diphenylamino)tetrakis[9,9-bis(*n*-butyl)fluorene], **OF(4)-NPh**: The Suzuki coupling procedure described above was followed using 9,9-bis(*n*-butyl)-2-diphenylamino-7-fluorenylboronic acid (367 mg, 0.75 mmol) and 2,2′-diiodo-bis[9,9-bis(*n*-butyl)fluorene] (202 mg, 0.25 mmol). The crude product was purified by column chromatography on silica gel using petroleum ether/dichloromethane (4:1, v/v) as eluent to afford a light-yellow solid (230 mg, 64% yield). ^{1}H NMR (400 MHz, $CDCl_3$, 25 °C): δ = 7.79–7.82 (m, 4H; ArH), 7.63–7.70 (m, 12H; ArH), 7.58–7.60 (m, 4H; ArH), 7.23–7.26 (m, 8H; ArH), 7.12–7.14 (m, 10H; ArH), 6.98–7.05 (m, 6H; ArH), 2.08–2.12 (m, 8H; CH_2), 1.88–1.96 (m, 8H; CH_2), 1.07–1.17 (m, 16H; CH_2), 0.70–0.77 ppm (m, 40H; CH_2CH_3); ^{13}C NMR (100 MHz, $CDCl_3$, 25 °C): δ = 152.4, 151.8, 151.4, 148.0, 147.1, 140.4, 140.3, 140.2, 140.0, 139.9, 139.6, 135.9, 129.1, 126.1, 126.0, 123.8, 123.5, 122.5, 121.4, 121.3, 121.2, 120.4, 119.9, 119.4, 55.2, 55.1, 40.2, 40.0, 26.1, 23.1, 23.0, 13.9, 13.8 ppm; MS (FAB): m/z: 1442.1 [M^+]; elemental analysis calcd (%) for $C_{108}H_{116}N_2$ (1440.9138): C 89.95, H 8.11, N 1.94; found: C 89.89, H 8.26, N 2.19.

Acknowledgements

This work was supported by Earmarked Research Grant (HKBU2051/01P) from the Research Grants Council, Hong Kong SAR, China. We gratefully acknowledge Dr. K. K. Shiu for his advice on the cyclic voltammetric measurements.

[1] R. H. Friend, R. W. Gymer, A. B. Holmes, J. H. Burroughes, R. N. Marks, C. Taliani, D. D. C. Bradley, D. A. Dos Santos, J. L. Brédas, M. Lögdlund, W. R. Salaneck, *Nature* **1999**, *397*, 121–128.
[2] J. L. Segura, N. Martin, *J. Mater. Chem.* **2000**, *10*, 2403–2453.
[3] K. Okumoyo, Y. Shirota, *Appl. Phys. Lett.* **2001**, *79*, 1231–1233.
[4] J. Shi, C. W. Tang, *Appl. Phys. Lett.* **2002**, *80*, 3201–3203.
[5] Y. Geng, S. W. Culligan, A. Trajkovska, J. U. Wallace, S. H. Chen, *Chem. Mater.* **2003**, *15*, 542–549.
[6] S. W. Culligan, Y. Geng, S. H. Chen, K. Klubek, K. M. Vaeth, C. W. Tang, *Adv. Mater.* **2003**, *15*, 1176–1179.
[7] K.-T. Wong, Y.-Y. Chien, R.-T. Chen, C.-F. Wang, Y.-T. Lin, H.-H. Chiang, P.-Y. Hsieh, C.-C. Wu, C. H. Chou, Y. O. Su, G.-H. Lee, S.-M. Peng, *J. Am. Chem. Soc.* **2002**, *124*, 11576–11577.
[8] M. Grell, D. D. C. Bradley, M. Inbasekaran, E. P. Woo, *Adv. Mater.* **1997**, *9*, 798–802.
[9] G. Klärner, J.-Y. Lee, V. Y. Lee, E. Chan, J.-P. Chen, A. Nelson, D. Markiewicz, R. Siemens, J. C. Scott, R. D. Miller, *Chem. Mater.* **1999**, *11*, 1800–1805.
[10] A. Donat-Bouillud, I. Lévesque, Y. Tao, M. D'Iorio, S. Beaupré, P. Blondin, M. Ranger, J. Bouchard, M. Leclerc, *Chem. Mater.* **2000**, *12*, 1931–1936.
[11] C. Ego, D. Marsitzky, S. Becker, J. Zhang, A. C. Grimsdale, K. Müllen, M. J. D. C. Silva, R. H. Friend, *J. Am. Chem. Soc.* **2003**, *125*, 437–443.
[12] D. Saninova, T. Miteva, H. G. Nothofer, U. Scherf, I. Glowacki, J. Ulanski, H. Fujikawa, D. Neher, *Appl. Phys. Lett.* **2000**, *76*, 1810–1812.
[13] T. Miteva, A. Meisel, W. Knoll, H. G. Nothofer, U. Scherf, D. C. Müller, K. Meerholz, A. Yasuda, D. Neher, *Adv. Mater.* **2001**, *13*, 565–570.
[14] C. Ego, A. C. Grimsdale, F. Uckert, G. Yu, G. Srdanov, K. Müllen, *Adv. Mater.* **2002**, *14*, 809–811.
[15] C. Adachi, K. Nagai, N. Tamoto, *Appl. Phys. Lett.* **1995**, *66*, 2679–2681.
[16] Y. Shirota, *J. Mater. Chem.* **2000**, *10*, 1–25.
[17] M. S. Wong, Z. H. Li, M. F. Shek, K. H. Chow, Y. Tao, M. D'Iorio, *J. Mater. Chem.* **2000**, *10*, 1805–1810.
[18] M. S. Wong, Z. H. Li, Y. Tao, M. D'Iorio, *Chem. Mater.* **2003**, *15*, 1198–1203.
[19] C. C. Kwok, M. S. Wong, *Macromolecules* **2001**, *34*, 6821–6830.
[20] C. C. Kwok, M. S. Wong, *Chem. Mater.* **2002**, *14*, 3158–3166.
[21] M. S. Wong, Z. H. Li, *Pure Appl. Chem.* **2004**, *76*, 1409–1419.
[22] W.-L. Yu, J. Pei, W. Huang, A. J. Heeger, *Adv. Mater.* **2000**, *12*, 828–831.
[23] Y. Geng, D. Katsis, S. W. Culligan, J. J. Ou, S. H. Chen, L. J. Rothberg, *Chem. Mater.* **2002**, *14*, 463–470.
[24] D. Katsis, Y. Geng, J. J. Ou, S. W. Culligan, A. Trajkovska, S. H. Chen, L. J. Rothberg, *Chem. Mater.* **2002**, *14*, 1332–1339.
[25] S. Setayesh, A. C. Grimsdale, T. Weil, V. Enkelmann, K. Müllen, F. Meghdadi, E. J. W. List, G. Leising, *J. Am. Chem. Soc.* **2001**, *123*, 946–953.
[26] D. Marsitzky, R. Vestberg, P. Blainey, B. T. Tang, C. J. Hawker, K. R. Carter, *J. Am. Chem. Soc.* **2001**, *123*, 6965–6972.
[27] H. C. Yeh, S. J. Yeh, C. T. Chen, *Chem. Commun.* **2003**, 2632–2633.
[28] K. Okumoto, Y. Shirota, *Chem. Mater.* **2003**, *15*, 699–707.

Received: November 16, 2004
Published online: March 22, 2005

